Journal of Photochemistry, 24 (1984) 207 - 222

KINETIC STUDIES OF Bi($6^4S_{3/2}$) BY TIME-RESOLVED ATOMIC RESONANCE FLUORESCENCE
I: REACTIONS WITH C_2H_2 (+He), N_2O AND FLUORESCENCE QUENCHING OF Bi($7^4P_{1/2}$)

CHARLES F. BELL and DAVID HUSAIN

Department of Physical Chemistry, The University of Cambridge, Lensfield Road, Cambridge CB2 1EP (Gt. Britain)

(Received August 3, 1983; in revised form September 21, 1983)

Summary

We present a kinetic study of ground state atomic bismuth Bi($6^4S_{3/2}$) generated by pulsed irradiation of $Bi(CH_3)_3$ in the presence of various gases and monitored with time-resolved atomic resonance fluorescence in the "single-shot" mode at $\lambda = 306.8$ nm (Bi($7^4P_{1/2}$) $\rightarrow$ Bi($6^4S_{3/2}$) + $h\nu$) following optical excitation. The third-order reaction Bi + C_2H_2 + He is studied in detail, including the effects of diffusion. The resulting third-order rate constant ($k_3 = (1.9 \pm 0.3) \times 10^{-33}$ cm^6 molecule^{-2} s^{-1} (300 K)) is compared with previous data, in particular those from time-resolved resonance absorption measurements. The absolute second-order rate constant for the reaction between Bi($6^4S_{3/2}$) and N_2O is also characterized ($k_2 = (2.1 \pm 0.4) \times 10^{-16}$ cm^3 molecule^{-1} s^{-1} (300 K)) and compared with previous upper limits reported for this reaction. Finally, the technique is applied to the study of fluorescence quenching of Bi($7^4P_{1/2}$) for which we report the following quenching cross sections σ^2 (Å^2) (errors, about 25%): N_2, 3.8; NO, 169; O_2, 570; N_2O, 164; CF_4, 12; C_2H_2, 97. These data are compared, where possible, with measurements of quenching cross sections derived from Stern–Volmer analyses on integrated plate intensities resulting from atomic emission following flash photolysis. The results from the two fundamentally different techniques are found to be in reasonable accord.

1. Introduction

Direct monitoring of group V elements in their $(np)^5$, $^4S_{3/2}$ electronic ground states, generated by pulsed irradiation and monitored with time-resolved atomic resonance fluorescence, has now been established for all the elements: Bi($6^4S_{3/2}$) [1], Sb($5^4S_{3/2}$) [2], As($4^4S_{3/2}$) [3], P($3^4S_{3/2}$) [4] and N($2^4S_{3/2}$) [5, 6]. These measurements lead to absolute rate data for the collisional behaviour of these ground states which are of fundamental

0047-2670/84/$3.00

interest [7 - 10]. The data may further be compared with results derived from time-resolved resonance absorption measurements on these atoms [11 - 15]. For $N(2^4S_{3/2})$ the main body of rate data has been determined by the experimentally more convenient and now standard spectroscopic marker technique employing the N + NO titration [16 - 22] although Morse and Kaufman [23] have demonstrated that resonance absorption measurements on $N(2^4S_{3/2})$ ($\lambda \approx 120$ nm, $N(3^4P_J) \leftarrow N(2^4S_{3/2})$) in a flow discharge system may still be used for rate measurements. The detection of resonance fluorescence under similar conditions has been reported by Becker *et al.* [24] but has not been employed to determine kinetic data. By contrast, Clyne and Ono [25] have recently employed resonance fluorescence measurements on $P(3^4S_{3/2})$ generated in a flow discharge system to determine absolute rate data for this atomic state. The earlier work on time-resolved resonance fluorescence measurements on $Bi(6^4S_{3/2})$ described by Husain *et al.* [1] was primarily concerned with establishing that time-resolved monitoring at λ = 306.8 nm ($Bi(7^4P_{1/2}) \rightarrow Bi(6^4S_{3/2}) + h\nu$) could be employed as a kinetic tool. The experimental arrangement involved a simple quartz reactor with the generation of $Bi(6^4S_{3/2})$ by a standard flash photolysis capillary discharge. The objective in those measurements was primarily to compare global decay rates of $Bi(6^4S_{3/2})$ in the presence of C_2H_2 and C_2H_4 at a given total pressure of buffer gas with kinetic data derived from resonance absorption, assuming overall third-order kinetic behaviour as initially derived from resonance absorption measurements [1]. The subsequent emphasis of the paper was to couple the time-resolved resonance fluorescence measurements with radiation trapping calculations using numerical solutions of the diffusion equation for radiation [26 - 28] and employing line shapes based on the summation of the Voigt profiles over the appropriate nuclear hyperfine components [29, 30].

In this paper we develop the experimental method for monitoring $Bi(6^4S_{3/2})$ with time-resolved resonance fluorescence in the "single-shot" mode to include a metallic reactor system with collection of light by a Cassegrain mirror, together with a high pressure pulsed discharge system. The resonance source employs a new type of microwave cavity, which was constructed in this laboratory following the recent design developed at the Philips Laboratories, Eindhoven. The use of this high intensity source for rate measurements with time-resolved resonance fluorescence monitoring constitutes the first application of its kind, to the best of our knowledge. The details of the third-order kinetic behaviour for $Bi + C_2H_2 + He$ are studied for the first time by the resonance fluorescence techniques, and we also describe absolute rate data for the reaction between $Bi(6^4S_{3/2})$ and N_2O, which has only been reported hitherto as a limit derived from resonance absorption measurements. Finally, we have succeeded in employing the method of time-resolved resonance fluorescence to obtain collisional quenching cross sections for $Bi(7^4P_{1/2})$ with a number of gases. These data can only be compared with the results of integrated plate intensity measurements resulting from atomic emission at λ = 306.8 nm subsequent to the flash photolysis of $Bi(CH_3)_3$ reported by Connor *et al.* [31].

2. Experimental details

The experimental arrangement for monitoring Bi($6\,^4S_{3/2}$) by time-resolved atomic resonance fluorescence measurements in the single-shot mode following the pulsed irradiation of Bi(CH_3)$_3$ involved a combination of aspects described for earlier measurements on Bi($6\,^4S_{3/2}$) [1], coupled with a number of those employed in analogous studies of Sb($5\,^4S_{3/2}$) [2] with various modifications. Figure 1 shows a block diagram of the apparatus. Figure 2 shows a cross section through the flash-lamp, reaction vessel and photomultiplier detection system. The pulse discharge itself involved significant modification to the magnetically pinched Garton–Wheaton source [32] used in previous measurements on Sb($5\,^4S_{3/2}$) [2]. The baffle system was removed and the discharge section of the lamp (Fig. 2) was designed to yield a high pressure, high intensity discharge through krypton (p_{Kr} = 1 atm; 8 kV; 10 μF; E = 320 J), initiated by means of high voltage switching using ignitron firing. Simultaneous triggering of the ignitron and the transient recorder (Data Laboratories DL 905), initiated by means of a mercury switch, was effected by the use of external triggering and a 300 V pulse from a standard delay unit. With this type of overall arrangement, even with photolysis through LiF optics ($\lambda > 105$ nm), photomultiplier gating (as in the work on Sb($5\,^4S_{3/2}$) [2]) was not necessary here. This is also, of course,

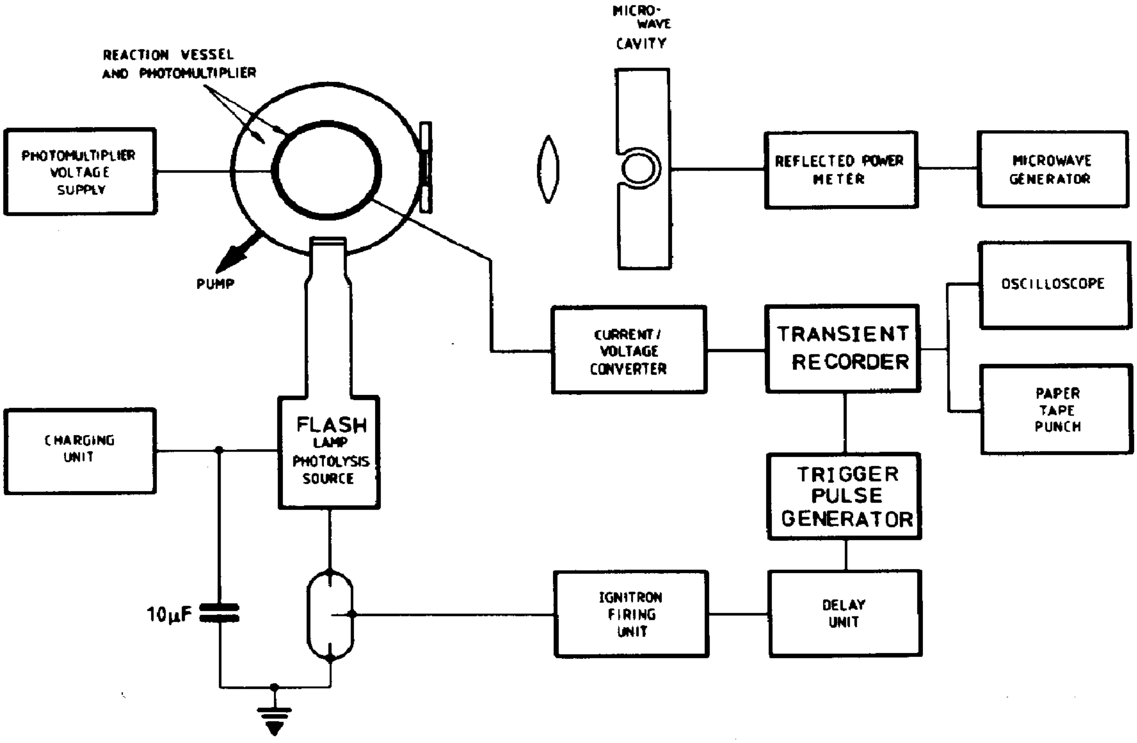

Fig. 1. Block diagram of the apparatus for the kinetic study of Bi($6\,^4S_{3/2}$) by time-resolved atomic resonance fluorescence.

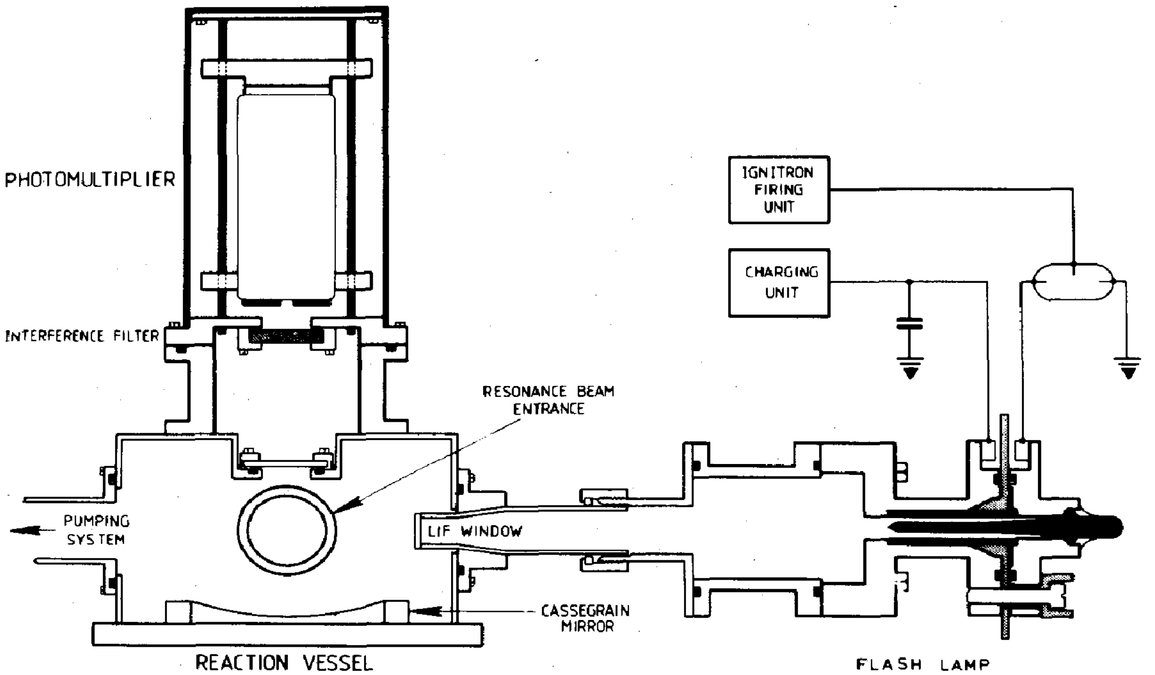

Fig. 2. Cross section through the flash-lamp, reaction vessel and photomultiplier detection system employed in the kinetic study of Bi($6^4S_{3/2}$) by time-resolved atomic resonance fluorescence.

due to the use of a high intensity atomic resonance source, lower transmission through the interference filter and the relatively long time scales over which Bi($6^4S_{3/2}$) is monitored (see later).

The resonance source was a microwave cavity of the type described by Beenakker [33, 34] and Beenakker and Boumans [35] coupled through a sealed quartz cylindrical capsule of outside diameter 6.2 mm containing sublimed BiI_3. The cavity of inside diameter 93.0 mm and internal height 10 mm was constructed of copper and operates in the TM_{010} mode. We have found that the emission is certainly more intense than the microwave-powered flow lamps for atomic bismuth used hitherto [1, 11], which followed the general design of Davis and Braun [36] and which employed a Fehsenfeld cavity [37]. Furthermore, this sealed system provides the further advantage of compactness and ease of optical optimization. The cavity was air cooled following Beenakker's design [33] and generally operated at about 75 W (microwave generator, EMS Microtron 200 mark 2 at 2450 MHz; reflected power, about 7 W).

The resonance fluorescence signal at $\lambda = 306.8$ nm (Bi($7^4P_{1/2}$) $\rightarrow$ Bi($6^4S_{3/2}$) + $h\nu$) following optical excitation of Bi($6^4S_{3/2}$) derived from the pulsed irradiation of $Bi(CH_3)_3$ was optically isolated by means of an interference filter (Oriel Corporation, U.S.A., type 521-3130; transmission at λ = 306.8 nm, about 8%; bandwidth at 50% peak transmission, about 12.4 nm) followed by photoelectric detection (EMI photomultiplier tube 9635 QB ("end-on") (Fig. 2); photomultiplier voltage, about 800 V; Brandenburg power supply 475 R, 0 - 2.2 kV). The photoelectric signals were amplified by means of a current-to-voltage converter [38] and transferred to the transient recorder, where the information was stored in digital form either for display on an oscilloscope or to be punched onto paper tape (Datadynamics 1133) for subsequent processing by the University of Cambridge IBM 3081 computer.

3. Materials

Most materials were prepared essentially as described in previous publications: helium, krypton, oxygen, NO, N_2O, CF_4, C_2H_2 and $BiMe_3$ [1, 11, 39, 40]. The purity of BiI_3 (Aldrich Chemicals Inc., U.S.A.; purity, 99.999%) and its careful sublimation under vacuum into the sealed quartz capsules used in the microwave cavity (see earlier) are critical for high spectral intensity at $\lambda = 306.8$ nm and operating lifetime. The purity of the $Bi(CH_3)_3$ and its concentration at low vapour pressures were difficult to ascertain precisely, but absorbance measurements in the UV were in reasonable accord with those reported by Connor *et al.* [31].

4. Results and discussion

Figure 3 gives an example of the digitized resonance fluorescence signal I_F against time at $\lambda = 306.8$ nm $(Bi(7\,^4P_{1/2}) \rightarrow Bi(6\,^4S_{3/2}) + h\nu)$, indicating the decay of ground state bismuth atoms generated by the pulsed irradiation

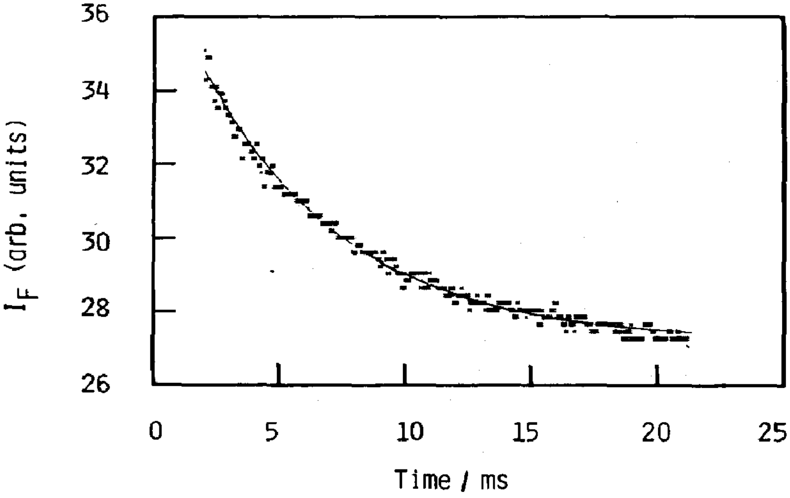

Fig. 3. Digitized time variation of the light intensity I_F at $\lambda = 306.8$ nm $(Bi(7\,^4P_{1/2}) \rightarrow Bi(6\,^4S_{3/2}))$ indicating the decay of resonance fluorescence due to ground state bismuth atoms generated by the pulsed irradiation of $Bi(CH_3)_3$ ($[Bi(CH_3)_3] = 8.7 \times 10^{14}$ molecules cm^{-3}; $[He] = 2.0 \times 10^{18}$ atoms cm^{-3}; $E = 320$ J): ×, data points; ——, computerized curve fitting to the form $I_F = \theta_1 + \theta_2 \exp(-k't)$.

of $Bi(CH_3)_3$ in the presence of excess helium buffer gas. The concentration of $Bi(CH_3)_3$ used in these studies, yielding densities of $Bi(6\,^4S_{3/2})$ suitable for resonance fluorescence in the single-shot mode, is primarily determined by the extinction coefficient ϵ_λ of this precursor and the geometry of the reactor shown in Fig. 2. The physical size of the reaction vessel is principally determined by the need to reduce scattered light from the photoflash-lamp. The actual size of the reaction volume is determined by the overlap of the cones of light from the flash-lamp, the resonance source and the light collection of the optics of the detection system. In approximate terms, for a given actinic wavelength due to the photoflash, for incident intensity I_0 at the LiF window, distance l ($\approx$ 7 cm) from the window to the centre of the reaction vessel, effective size of the reaction space l' ($l' \ll l$) and using the weak light absorption approximation for actinic radiation at the centre of the vessel, then the rate of production of $Bi(6\,^4S_{3/2})$ is $I_0 \exp(-\epsilon cl)\, \epsilon cl'$. This is maximized at a $Bi(CH_3)_3$ concentration c of $1/\epsilon l$. The concentration of $Bi(CH_3)_3$ indicated in Fig. 3 is sensibly consistent with the data on the extinction coefficient for $Bi(CH_3)_3$ given by Connor *et al.* [31]. Ideally, the quantity $\int I_0(\lambda) \exp(-\epsilon cl)\, \epsilon cl'$ should be optimized over both ϵ_λ and the light output of the flash-lamp. Christie and Porter [41] have shown that a classical photoflash-lamp can be approximated to a black body of temperature of about 6500 °C, but this would be an even cruder approximation for a spark discharge of the type shown in Fig. 2.

It has been shown in the initial resonance fluorescence studies on $Bi(6\,^4S_{3/2})$ [1] that the time-dependent fluorescence intensity $I_F(\lambda = 306.8\ \text{nm})$ is given by

$$I_F = \frac{\phi[Bi(6\,^4S_{3/2})]_{t=0} \exp(-k't)}{1 + \Sigma k_Q[Q]/A_{nm}} \tag{1}$$

where k' is the first-order decay coefficient for the removal of $Bi(6\,^4S_{3/2})$ and is generally the term from which kinetic information is extracted. A_{nm} is the Einstein coefficient for the transition $Bi(7\,^4P_{1/2}) \rightarrow Bi(6\,^4S_{3/2}) + h\nu$ at $\lambda = 306.8$ nm and is taken to be $1.7 \times 10^8\ s^{-1}$ ($\tau_e = 5.9$ ns) in these studies following Cunningham and Link [42]. The term $\Sigma k_Q[Q]$ represents the total first-order removal coefficient for fluorescence quenching of $Bi(7\,^4P_{1/2})$ and ϕ combines all the appropriate terms that are involved in the light absorption process from the resonance source together with the efficiency of the light collection system and amplification. Radiation trapping calculations on the $\lambda = 306.8$ nm transition [1] have demonstrated that A_{nm}, as used in eqn. (1), is itself really a function of time as $[Bi(6\,^4S_{3/2})] = f(t)$ and τ^*/τ_e (where $\tau^* = f[Bi(6\,^4S_{3/2})]$ is the effective radiative lifetime of $Bi(7\,^4P_{1/2}) \rightarrow Bi(6\,^4S_{3/2})$). However, the exponential term dominates the time profile of I_F (see later) and A_{nm} is taken to be the above constant in a kinetic decay. As hitherto [1 - 4, 6], account is taken of the steady scattered stray light from the resonance source and the fluorescence intensity is fitted by computer analysis to the form

$$I_F = \theta_1 + \theta_2 \exp(-k't) \tag{2}$$

It was found to be computationally convenient to fit $I_F(t)$ in eqn. (2) to the "Lamfit" procedure of Powell [43] to obtain values of θ_1, as this property is independent of the units of time employed. Subsequently, the second term in eqn. (2) is characterized by the use of a standard regression of $\ln(I_F - \theta_1)$ on t. The full curve in Fig. 3 shows the result of this type of curve fitting to a decay trace. All data were analysed in this way. Finally, a linearity check of θ_2 with $[BiMe_3]$, which is in turn assumed to be a linear function of $[Bi(6^4S_{3/2})]_{t=0}$, was made as described in the earlier time-resolved resonance fluorescence investigation on $Bi(6^4S_{3/2})$ [1].

4.1. $Bi + C_2H_2 + He$

The collisional removal of $Bi(6^4S_{3/2})$ by C_2H_2 was investigated first to compare the results of the present system with those reported from the earlier resonance fluorescence investigations [1] where third-order kinetics were assumed following the studies by time-resolved resonance absorption [11]. Thus, those initial studies were all performed at a fixed total pressure p_{He} of 5.3 kN m^{-2} [1]. By contrast, the present measurements describe the decay of $Bi(6^4S_{3/2})$ with varying p_{He} where the contribution by diffusional removal of the atom is also extracted. Figure 4 shows examples of the curve fitting of measured resonance fluorescence decays for $Bi(6^4S_{3/2})$ in the form of $(I_F - \theta_1)$ *versus* t (see earlier) for (a) fixed [He] and various $[C_2H_2]$ and (b) fixed $[C_2H_2]$ and various [He]. The varying intercepts of such curves primarily arise from the effects of fluorescence quenching which affects the values of θ_2 (see later). These intercepts are also considerably more sensitive to variations in the light output from both the pulsed source and the high intensity resonance source than are the values of k', the first-order decay coefficient for $Bi(6^4S_{3/2})$. Hence, fluorescence quenching data in particular must be derived from sets of measurements in which the required constancy in these light outputs is more restrictive than is the case for the determination of k' (see later). k' can be expressed in the form

$$\frac{-\mathrm{d}(\ln[Bi(6^4S_{3/2})])}{\mathrm{d}t} = k'$$

$$= K + \frac{\beta}{p_{He}} + k_3[C_2H_2][He] \qquad (3)$$

K represents the first-order contributions to the removal of $Bi(6^4S_{3/2})$ by $Bi(CH_3)_3$ and photolysis fragments which were found by variation in $[Bi(CH_3)_3]$ to be negligible in comparison with the magnitudes of the other terms in eqn. (3), equal to about 50 s^{-1} and usually less, and often difficult to detect. This is in full accord with observations made previously by Husain *et al.* [1]. Thus we may simplify eqn. (3) to the form

$$\frac{k'}{p_{He}} = \alpha + \frac{\beta}{p_{He}^2} \qquad (4)$$

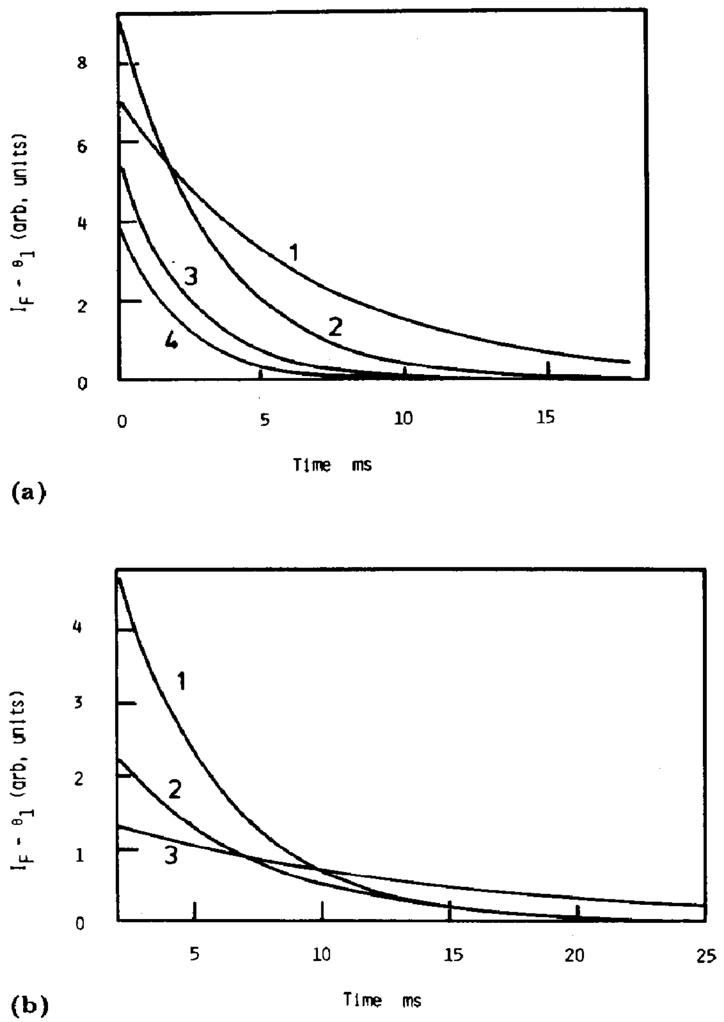

Fig. 4. Computerized curve fitting of the experimental intensity profiles for the decay of $Bi(6\,^4S_{3/2})$ obtained by time-resolved atomic resonance fluorescence at $\lambda = 306.8$ nm ($Bi(7\,^4P_{1/2}) \rightarrow Bi(6\,^4S_{3/2})$) ($(I_F - \theta_1)$ *vs.* t) in the presence of C_2H_2 and He: (a) $[He] = 1.38 \times 10^{18}$ atoms cm^{-3}, $[Bi(CH_3)_3] = 9.6 \times 10^{13}$ molecules cm^{-3} (curve 1, $[C_2H_2] = 0$; curve 2, $[C_2H_2] = 2.0 \times 10^{16}$ molecules cm^{-3}; curve 3, $[C_2H_2] = 7.0 \times 10^{16}$ molecules cm^{-3}; curve 4, $[C_2H_2] = 7.7 \times 10^{16}$ molecules cm^{-3}); (b) $[C_2H_2] = 3.0 \times 10^{16}$ molecules cm^{-3}, $[Bi(CH_3)_3] = 2.1 \times 10^{14}$ molecules cm^{-3} (curve 1, $[He] = 2.5 \times 10^{17}$ atoms cm^{-3}; curve 2, $[He] = 4.3 \times 10^{17}$ atoms cm^{-3}; curve 3, $[He] = 180 \times 10^{17}$ atoms cm^{-3}).

where α is directly related to the term $k_3[C_2H_2]$ and β is related to the diffusion coefficient of the atom. Unfortunately, the actual diffusion coefficient could not be determined explicitly as, for instance, by the "long-time solution" of the diffusion equation [28, 44] since the effective geometry of the reaction volume is unknown. However, the slope of plots based on eqn. (4) can be used for empirical corrections for the effects of diffusion of $Bi(6\,^4S_{3/2})$ from the reaction volume. The intercept of the same plot can yield k_3 at a given $[C_2H_2]$.

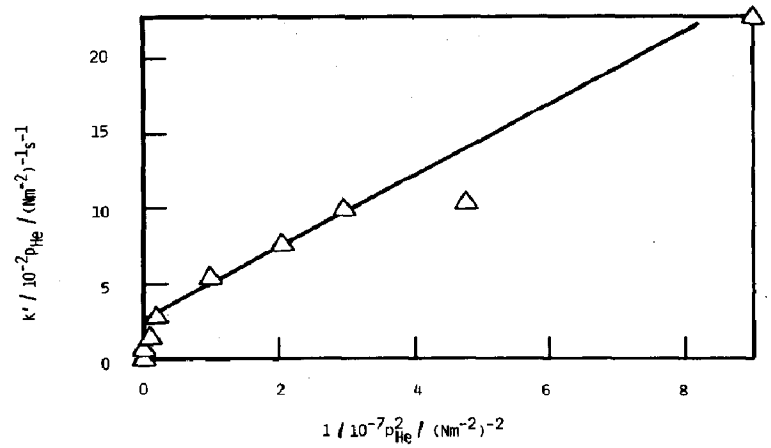

Fig. 5. Variation in the pseudo-first-order rate coefficient k' for the decay of Bi($6^4S_{3/2}$) in the presence of C_2H_2 and He (k'/p_{He} *vs.* $1/p_{He}^2$) indicating the effects of both third-order kinetics and diffusion ($[Bi(CH_3)_3] = 2.1 \times 10^{14}$ molecules cm^{-3}; $[C_2H_2] = 3.0 \times 10^{16}$ molecules cm^{-3}; $E = 320$ J).

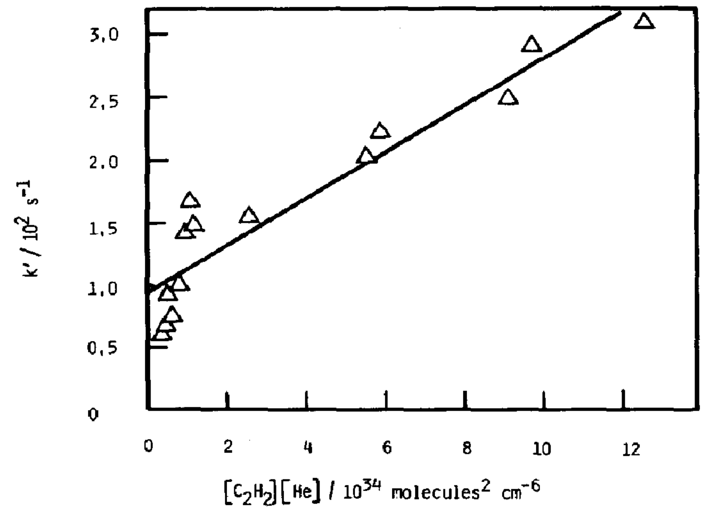

Fig. 6. Variation in the pseudo-first-order rate coefficient k' (diffusion corrected) for the decay of Bi($6^4S_{3/2}$) in the presence of C_2H_2 and He ($[Bi(CH_3)_3] = 2.1 \times 10^{14}$ molecules cm^{-3}).

Figure 5 gives an example of a plot based on eqn. (4) using a fixed pressure of C_2H_2. Figure 6 shows the plot of k' (diffusion corrected) *versus* $[C_2H_2][He]$ (eqn. (3)). The slope of this plot yields the value $k_3(Bi + C_2H_2 + He) = (1.9 \pm 0.3) \times 10^{-33}$ cm^6 $molecule^{-2}$ s^{-1} (300 K; 2σ). This is marginally lower, at best by about 25% within the error limits, than the third-order rate constant from the measurements at a single pressure of helium of $k_3 = (3.4 \pm 0.3) \times 10^{-33}$ cm^6 $molecule^{-2}$ s^{-1} (300 K; 1σ) reported by Husain *et al.* [1]. The result can also be compared with that derived from resonance absorption measurements [11] of $k_3 = (1.1 \pm 0.3) \times 10^{-33}$ cm^6 $molecule^{-2}$ s^{-1}

(300 K; 1σ). We have shown that rate data derived from the combination of resonance absorption and resonance fluorescence measurements [1 - 4, 11 - 15] can be used to determine γ in the modified Beer–Lambert law [45]:

$$I_{tr} = I_0 \exp\{(-\epsilon cl)^{\gamma}\} \qquad (5)$$

The factor γ has not been determined either by empirical [45] or by direct techniques for the atomic bismuth transition at $\lambda = 306.8$ nm. For a given rate constant determined by both resonance absorption and resonance fluorescence $k_R{}^{\text{res abs}}/k_R{}^{\text{res fluor}} = \gamma$. Thus, a comparison of the present result for k_3 and that of Husain *et al.* [1] with the resonance absorption data [11] yields respectively $\gamma(\lambda = 306.8\ \text{nm}) = 0.56 \pm 0.13$ (2σ) and $\gamma(\lambda = 306.8\ \text{nm}) = 0.32 \pm 0.19$ (2σ).

4.2. *Bi + N_2O*

The collisional removal of Bi($6\,^4S_{3/2}$) by N_2O has not been previously investigated by time-resolved resonance fluorescence. Resonance absorption measurements [11] yielded upper limits for k_2(Bi + N_2O) of less than 2.5×10^{-16} cm^3 molecule^{-1} s^{-1} and less than 3.1×10^{-16} cm^3 molecule^{-1} s^{-1} at $T = 320$ K and $T = 340$ K respectively. As has been emphasized hitherto [11], this represents the sum of two symmetry-allowed exothermic processes on the basis of (J,Ω) coupling [7]:

$$\text{Bi}(6\,^4S_{3/2}) + N_2O(X\,^1\Sigma^+) \xrightarrow[E_{1/2}]{k_{2a}} \text{BiO}(X\,^2\Pi_{1/2}) + N_2(X\,^1\Sigma_g^+)$$

($\Delta H = -1.64$ eV [46 - 48]) and

$$\text{Bi}(6\,^4S_{3/2}) + N_2O(X\,^1\Sigma^+) \xrightarrow[E_{1/2}]{k_{2b}} \text{BiO}(X\,^2\Pi_{3/2}) + N_2(X\,^1\Sigma_g^+)$$

($\Delta H = -0.65$ eV [46 - 48]). However, there are many symmetry-allowed exothermic oxygen atom abstraction processes by a range of atoms reacting with N_2O [9, 10] whose low rates result from energy barriers associated with the 18-electron closed shell structure of this molecule. This reaction is investigated further here.

Figure 7 shows examples of the numerical fitting by computer of the resonance fluorescence profiles at $\lambda = 306.8$ nm (($I_F - \theta_1$) *versus* t) for various concentrations of N_2O. In this set of experiments, the magnitude of K (eqn. (3)) was sufficiently large in relation to the competing terms for its contribution to k' to be included. Figure 8 shows the result of the values of k', which have been corrected for diffusion and K, *versus* [N_2O], constrained to pass through the origin. The slope of Fig. 8 yields k_2(Bi + N_2O) (= $k_{2a} + k_{2b}$) = $(2.1 \pm 0.4) \times 10^{-16}$ cm^3 molecule^{-1} s^{-1} (300 K; 2σ).

4.3. *Fluorescence quenching of Bi $7\,^4P_{1/2}$*

Whilst, in principle, time-resolved resonance fluorescence studies can be used to determine fluorescence quenching of the emitting state through the use of eqn. (1), this type of measurement is rarely reported for two main

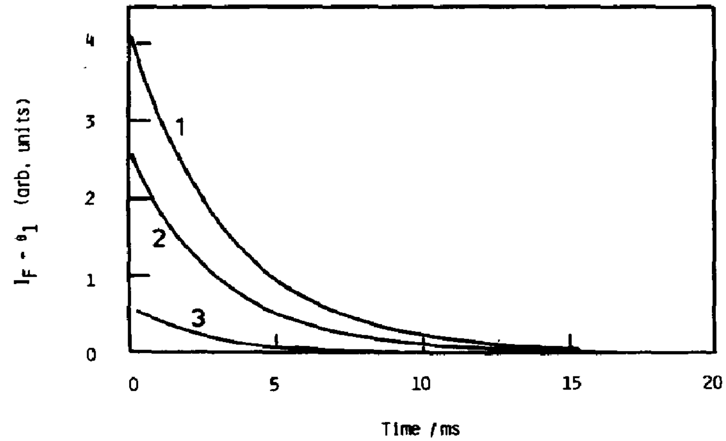

Fig. 7. Computerized curve fitting of experimental intensity profiles for the decay of $Bi(6^4S_{3/2})$ obtained by time-resolved atomic resonance fluorescence at $\lambda = 306.8$ nm ($Bi(7^4P_{1/2}) \rightarrow Bi(6^4S_{3/2})$) ($(I_F - \theta_1)$ *vs.* t) in the presence of various concentrations of N_2O: curve 1, $[N_2O] = 4.9 \times 10^{17}$ molecules cm^{-3}; curve 2, $[N_2O] = 7.8 \times 10^{17}$ molecules cm^{-3}; curve 3, $[N_2O] = 9.6 \times 10^{17}$ molecules cm^{-3}.

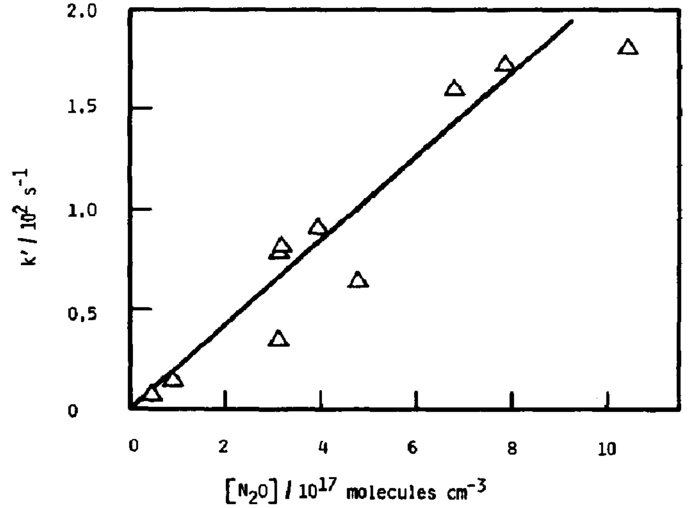

Fig. 8. Variation in the pseudo-first-order rate coefficient k' (diffusion corrected and normalized) for the decay of $Bi(6^4S_{3/2})$ in the presence of N_2O.

reasons. Often the term $\Sigma k_Q[Q]/A_{nm}$ is very small compared with unity and is consequently difficult to measure. Secondly, this type of measurement requires an accuracy in the reproducibility of θ_2 (eqn. (2)) which is not required for comparably accurate values of k'. In practice, a small variation in $[Bi(6^4S_{3/2})]_{t=0}$ through a variation, for example, in the light output of the photoflash-lamp, would only cause a change in the magnitude of $I_F(\lambda = 306.8$ nm) but would have no significant effect on the slope of a plot of $\ln I_F$ *versus* t on the basis of eqn. (1). Nevertheless, although the data are scattered, for the above-stated reasons, we have determined fluorescence

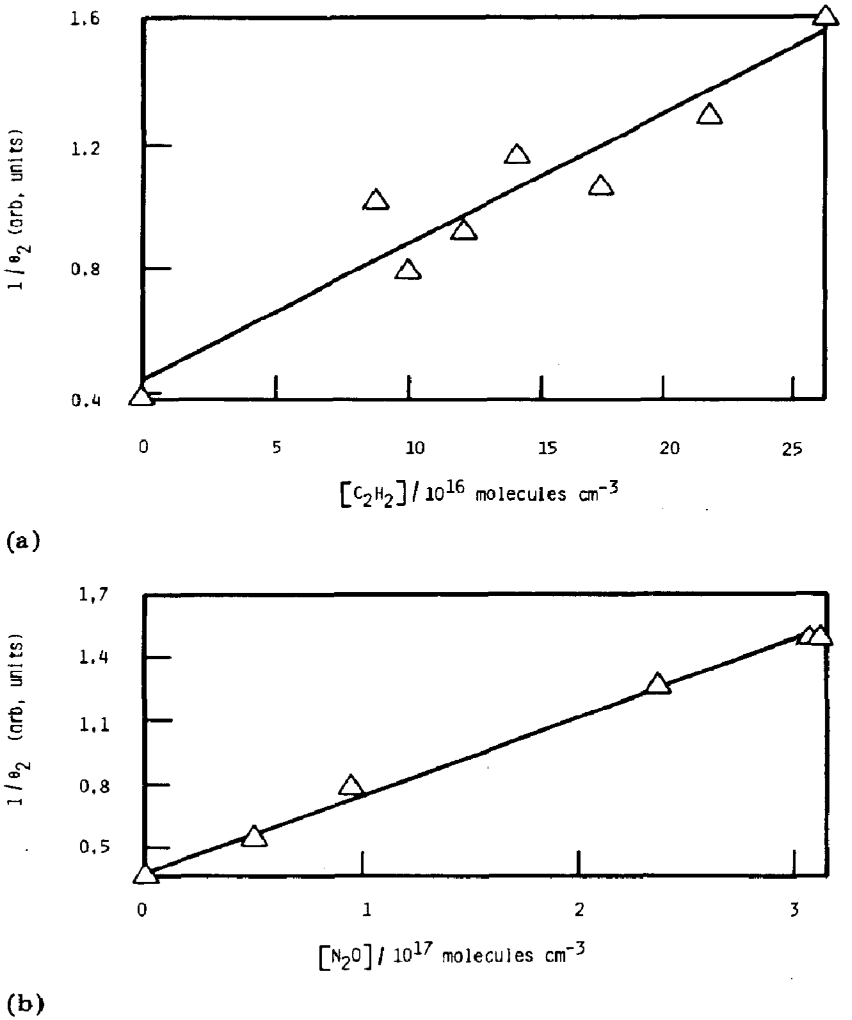

Fig. 9. Stern–Volmer plots ($1/\theta_2$ *vs.* [Q]) for the collisional quenching of Bi($7\,^4P_{1/2}$) by (a) C_2H_2 and (b) N_2O obtained by time-resolved atomic resonance fluorescence measurements on Bi($6\,^4S_{3/2}$) at $\lambda = 306.8$ nm ($7\,^4P_{1/2}$–$6\,^4S_{3/2}$) following the flash photolysis of $Bi(CH_3)_3$: (a) $[Bi(CH_3)_3] = 2.6 \times 10^{14}$ molecules cm^{-3}, [He] $= 1.2 \times 10^{18}$ atoms cm^{-3}, $E = 320$ J; (b) $[Bi(CH_3)_3] = 3.6 \times 10^{14}$ molecules cm^{-3}, $[N_2] = 3.8 \times 10^{17}$ molecules cm^{-3}, $E = 320$ J.

quenching data for Bi($7\,^4P_{1/2}$) in these measurements through the use of eqns. (1) and (2). This includes fluorescence quenching by molecules involved in atom–molecule recombination studies (with NO and O_2) for Bi($6\,^4S_{3/2}$) in a subsequent paper [49].

Given that values of θ_2 result from analyses of the data in the form of eqn. (2), it clearly can be seen from eqn. (1) that the ratio of the slope to the intercept of $1/\theta_2$ *versus* [Q] yields $\Sigma k_Q[Q]/A_{nm}$ for a given mixture. Thus, using the value of A_{nm} reported by Cunningham and Link [42] of 1.7×10^8 s^{-1} and following the procedure of Connor *et al.* [31] of employing this value in the Stern–Volmer analyses, we may determine fluorescence

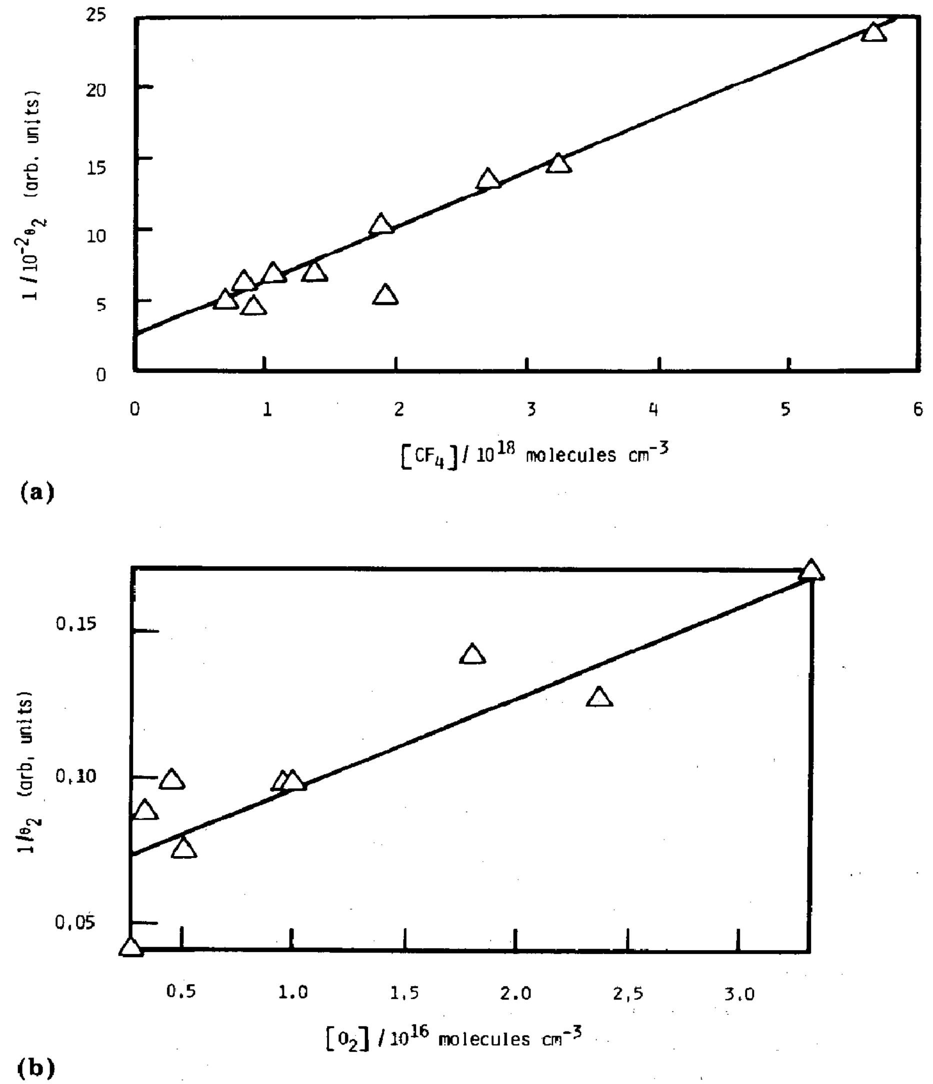

Fig. 10. Stern–Volmer plots ($1/\theta_2$ *vs.* [Q]) for the collisional quenching of Bi($7\,^4P_{1/2}$) by (a) CF_4 and (b) O_2 obtained by time-resolved atomic resonance fluorescence measurements on Bi($6\,^4S_{3/2}$) at $\lambda = 306.8$ nm ($7\,^4P_{1/2}$–$6\,^4S_{3/2}$) following the flash photolysis of $Bi(CH_3)_3$: (a) $[Bi(CH_3)_3] = 2.3 \times 10^{14}$ molecules cm^{-3}, $[NO] = 2.3 \times 10^{16}$ molecules cm^{-3}, $E = 320$ J; (b) $[Bi(CH_3)_3] = 4.8 \times 10^{13}$ molecules cm^{-3}, $[He] = 7.1 \times 10^{17}$ atoms cm^{-3}, $E = 320$ J.

quenching data for the $7\,^4P_{1/2}$ state. Figures 9 and 10 show examples of Stern–Volmer plots for the gases C_2H_2, N_2O, CF_4 and O_2. A variation of four to five was observed in the values of θ_2 across the range of [Q] investigated. No significant effect of quenching by helium was observed. For mixtures of quenching gases Q_1 and Q_2 (as in Figs. 9 and 10) characterized respectively by collisional quenching constants k_{Q_1} and k_{Q_2}, the following procedure was adopted. We may readily show that for a fixed value of $[Q_1]$ the ratio of the

TABLE 1

Collision cross sections for quenching of Bi($7^4P_{1/2}$) by various gases Q derived from time-resolved atomic resonance fluorescence measurements at $\lambda = 306.8$ nm (Bi($7^4P_{1/2}$) $\rightarrow$ Bi($6^4S_{3/2}$) + $h\nu$)

Q	σ^2 (Å^2)[a]	σ^2 (Å^2)[b]
N_2	3.8	< 3.5
NO	169	—
O_2	570	110
N_2O	164	—
CO_2	—	620
CF_4	12	—
C_2H_2	97	—
C_2H_4	—	330

[a] This work (time-resolved resonance fluorescence).

[b] Integrated plate intensity measurements of atomic emission following flash photolysis (from ref. 31).

slope to the intercept of a plot of $1/\theta_2$ *versus* $[Q_2]$ is given by $k_{Q_2}/(A_{nm} + k_{Q_1}[Q_1])$ following eqns. (1) and (2). Hence, k_{Q_2} may be determined using the value of k_{Q_1} derived from an experiment involving Q_1 alone. Alternatively, the above result may be combined with an analogous procedure, plotting $1/\theta_2$ *versus* $[Q_1]$ to yield $k_{Q_1}/(A_{nm} + k_{Q_2}[Q_2])$ hence giving rise to two simultaneous equations from which k_{Q_1} and k_{Q_2} may be calculated. The results are given in Table 1 in the form of cross sections σ^2 (Å^2) for direct comparison with the results of Connor *et al.* [31].

The errors assigned to our data are typically about 30%, simply on account of the scatter in the values of θ_2 for the reasons given above. Owing to the neglect of possible radiation trapping in their analyses, Connor *et al.* [31] describe their data as upper limits. For comparison of the data from the two sets of measurements, brief consideration must be given to the method of Connor *et al.* [31]. Essentially, their cross sections are obtained from measurements of integrated plate intensities of atomic lines recorded following the flash photolysis of $Bi(CH_3)_3$ in the presence of various gases with the assumption that the total line intensity from emission over the complete profile, there being no time resolution, satisfies a plate calibration made with white light. Considering the large fundamental differences in techniques, the agreement between the data is sensible, particularly in demonstrating the effects of large cross sections (*e.g.* O_2, N_2O and CO_2, C_2H_2 and C_2H_4 (Table 1)).

Acknowledgments

We are indebted to Mr. D. G. Oliver and his colleagues of the engineering workshops of the department for the construction of the microwave cavity and to Mr. C. J. Smith of the glass blowing department of this laboratory for the construction of the sealed capsules.

References

1 D. Husain, L. Krause and N. K. H. Slater, *J. Chem. Soc., Faraday Trans. II, 73* (1977) 1678.
2 D. Husain, L. Krause and N. K. H. Slater, *J. Chem. Soc., Faraday Trans. II, 73* (1977) 1706.
3 D. Husain and N. K. H. Slater, *J. Chem. Soc., Faraday Trans. II, 74* (1978) 1222.
4 D. Husain and N. K. H. Slater, *J. Chem. Soc., Faraday Trans. II, 74* (1978) 1627.
5 J. H. Lee, J. V. Michael, W. A. Payne and L. J. Stief, *J. Chem. Phys., 69* (1978) 3069.
6 D. Husain and N. K. H. Slater, *J. Chem. Soc., Faraday Trans. II, 76* (1980) 606.
7 D. Husain, *Ber. Bunsenges. Phys. Chem., 81* (1977) 168.
8 R. J. Donovan and D. Husain, *Chem. Rev., 70* (1970) 489.
9 R. J. Donovan and D. Husain, *Annu. Rep. Prog. Chem., Sect. A, 68* (1971) 123.
10 R. J. Donovan, D. Husain and L. J. Kirsch, *Annu. Rep. Prog. Chem., Sect. A, 69* (1972) 19.
11 D. Husain and N. K. H. Slater, *J. Photochem., 6* (1977) 325.
12 D. Husain and N. K. H. Slater, *J. Photochem., 7* (1977) 59.
13 D. Husain and P. E. Norris, *J. Chem. Soc., Faraday Trans. II, 73* (1977) 1815.
14 D. Husain and P. E. Norris, *J. Chem. Soc., Faraday Trans. II, 73* (1977) 415.
15 D. Husain and P. E. Norris, *J. Chem. Soc., Faraday Trans. II, 73* (1977) 1107.
16 A. Nelson Wright and C. A. Winkler, *Active Nitrogen*, Academic Press, New York, 1968.
17 I. M. Campbell and B. A. Thrush, *Annu. Rep. Prog. Chem., 62* (1965) 17.
18 B. Brocklehurst and K. R. Jennings, *Prog. React. Kinet., 4* (1967) 1.
19 G. G. Manella, *Chem. Rev., 63* (1963) 1.
20 K. R. Jennings and J. W. Linnett, *Q. Rev., Chem. Soc., 12* (1958) 116.
21 M. F. Golde and B. A. Thrush, *Rep. Prog. Phys., 36* (1973) 1285.
22 B. A. Thrush, *Annu. Rev. Phys. Chem., 19* (1968) 371.
23 F. A. Morse and F. Kaufman, *J. Chem. Phys., 42* (1965) 1785.
24 K. H. Becker, W. Groth and W. Jud, *Z. Naturforsch., 24a* (1969) 1953.
25 M. A. A. Clyne and Y. Ono, *J. Chem. Soc., Faraday Trans. II, 78* (1982) 1149.
26 E. A. Milne, *J. London Math. Soc., 1* (1926) 40.
27 R. P. Blickensderfer, W. H. Breckenridge and J. Simons, *J. Chem. Phys., 80* (1976) 653.
28 A. C. G. Mitchell and M. W. Zemansky, *Resonance Radiation and Excited Atoms*, Cambridge University Press, London, 1934.
29 W. Gordy, W. A. Smith and R. F. Trambarulo, *Microwave Spectroscopy*, Dover Publications, New York, 1960.
30 P. C. Magnante and H. H. Stroke, *J. Opt. Soc. Am., 59* (1969) 83.
31 J. Connor, P. J. Young and O. P. Strausz, *J. Am. Chem. Soc., 93* (1971) 822.
32 W. R. S. Garton, *J. Sci. Instrum., 36* (1959) 11.
33 C. I. M. Beenakker, *Spectrochim. Acta, Part B, 31* (1976) 483.
34 C. I. M. Beenakker, *Spectrochim. Acta, Part B, 32* (1977) 173.
35 C. I. M. Beenakker and P. W. J. M. Boumans, *Spectrochim. Acta, Part B, 33* (1978) 53.
36 D. D. Davis and W. Braun, *Appl. Opt., 7* (1968) 2071.
37 F. C. Fehsenfeld, K. M. Evenson and H. P. Broida, *Rev. Sci. Instrum., 36* (1965) 294.
38 W. H. Wing and T. M. Sanders, Jr., *Rev. Sci. Instrum., 33* (1962) 1341.
39 M. A. A. Chowdhury and D. Husain, *J. Chem. Soc., Faraday Trans. II, 74* (1978) 1065.
40 D. Husain and J. Schifino, *J. Chem. Soc., Faraday Trans. II, 78* (1982) 2083.

41 M. I. Christie and G. Porter, *Proc. R. Soc. London, Ser. A, 212* (1952) 398.

42 P. T. Cunningham and J. K. Link, *J. Opt. Soc. Am., 47* (1967) 1000.

43 M. J. D. Powell, personal communication, 1979, cited in D. Husain and N. K. H. Slater, *J. Chem. Soc., Faraday Trans. II, 76* (1980) 606.

44 M. W. Zemansky, *Phys. Rev., 34* (1929) 213.

45 R. J. Donovan, D. Husain and L. J. Kirsch, *Trans. Faraday Soc., 66* (1970) 2551.

46 K. P. Huber and G. Herzberg, *Molecular Spectra and Molecular Structure*, Vol. IV, *Constants of Diatomic Molecules*, Van Nostrand Reinhold, New York, 1979.

47 A. G. Gaydon, *Dissociation Energies and Spectra of Diatomic Molecules*, Chapman and Hall, London, 1968.

48 G. Herzberg, *Molecular Spectra and Molecular Structure*, Vol. III, *Electronic Structure of Polyatomic Molecules*, Van Nostrand Reinhold, New York, 1966.

49 C. F. Bell and D. Husain, *J. Photochem., 24* (1984) 223.